Additive color mixture of emission from InGaN/GaN quantum wells on structure-controlled GaN microfacets

M. Ueda, T. Kondou, K. Hayashi, M. Funato,[a] and Y. Kawakami
Department of Electronic Science and Engineering, Kyoto University, Kyoto 615-8510, Japan

Y. Narukawa and T. Mukai
Nitride Semiconductor Research Laboratory, Nichia Corporation, Tokushima 774-8601, Japan

(Received 9 November 2006; accepted 26 March 2007; published online 24 April 2007)

Altering the mask geometry controls the apparent emission color from InGaN/GaN quantum wells (QWs) grown on GaN microfacets formed by regrowth on SiO_2 mask stripes over a wide spectral range, including white. The mask stripes are along the $\langle 1\bar{1}00\rangle$ direction and the microfacet structure is composed of the (0001) and $\{11\bar{2}2\}$ planes. With a large occupancy of the mask opening within a period, both facets simultaneously appear and emit different colors. For example, the $\{11\bar{2}2\}$ facet QWs emit blue and the (0001) facet QWs emit green. On the other hand, with a small occupancy of the mask opening, the $\{11\bar{2}2\}$ facets become dominant and a greenish-blue light is emitted. To synthesize these spectra, the mask patterns are designed so that two different microfacet structures are included within a period. Hence, the macroscopically observed emission color, which depends on the pattern design, can change from green to purple through white due to the additive color mixture. © *2007 American Institute of Physics*. [DOI: 10.1063/1.2731526]

White light emitting diodes (LEDs) based on InGaN/GaN quantum wells (QWs) have attained great success in solid-state lighting.[1] Because semiconductor emitters inherently provide nearly monochromatic output light, current white LEDs consist of a blue LED pumping a yellow phosphor. A drawback to using phosphors is that the absorption energy of a phosphor must agree with the emission energy of the LED, which limits the material and consequently, the spectral design. Furthermore, the Stokes loss due to the downconversion from blue to yellow is inevitable.

To circumvent these issues, all semiconductor optical devices emitting arbitrary colors, including pastels and white, are quite attractive. Recently, we demonstrated that InGaN/GaN QWs grown on three-dimensional GaN microfacet structures formed by a regrowth technique exhibit a facet-dependent In composition and InGaN thickness.[2–4] Consequently, each facet QW produces a different emission color. Because changing the In composition can tune the band gap energy of InGaN from 0.7 eV (InN) (Refs. 5 and 6) to 3.5 eV (GaN), the microfacet InGaN/GaN QWs can be single-chip multiwavelength light emitters, which can control the color. Herein, we propose to design mask patterns for the regrowth so that different microfacet structures form within a tiny region (<100 μm) to produce arbitrary colors by the additive color mixture of the emission from each microfacet QW.

The samples were grown on sapphire (0001) substrates using low-pressure (300 Torr) metal organic vapor phase epitaxy. Initially, ~ 3 μm GaN layers were grown. Then a 100-nm-thick SiO_2 layer was deposited as a mask material by plasma enhanced chemical vapor deposition. The mask stripes were formed along the $\langle 1\bar{1}00\rangle$ direction by conventional photolithography. Three different mask geometries were prepared; the dimensions of (window, mask) were (15 μm, 5 μm), (5 μm, 5 μm), and (5 μm, 15 μm), which are denoted as patterns A, B, and C, respectively. Similar to Refs. 7–9, subsequent regrowth of GaN created microstructures composed of (0001) and $\{11\bar{2}2\}$ facets along the $\langle 1\bar{1}00\rangle$ direction. Finally, InGaN/GaN five-period QWs were fabricated on these microfacets. The macroscopic optical properties were assessed by photoluminescence (PL) measurements at room temperature (RT). The excitation source was a He–Cd laser (325 nm) with an excitation density of 63.5 W/cm^2. Microscopically, cathodoluminescence (CL) measurements were conducted at RT with an acceleration voltage of 5 kV.

Figure 1 shows cross sectional images of the microfacet

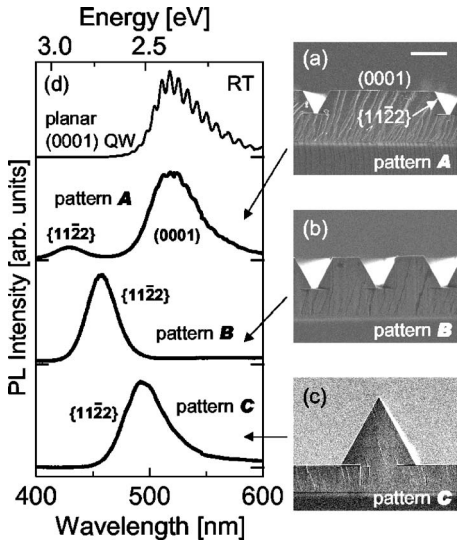

FIG. 1. Cross sectional SEM images of InGaN/GaN microfacet QWs grown on (a) pattern A [(window, mask)=(15 μm, 5 μm)], (b) pattern B [(5 μm, 5 μm)], and (c) pattern C [(5 μm, 15 μm)]. The scale bar [in (a)] represents 5 μm. (d) RT-PL spectra of these microfacet QWs as well as a simultaneously grown planar (0001) QW.

[a]Electronic mail: funato@kuee.kyoto-u.ac.jp

QWs acquired by scanning electron microscopy (SEM) and their PL spectra at RT. It should be noted that all the samples discussed in Fig. 1 were simultaneously fabricated. Figures 1(a)–1(c) confirm that all the structures are composed of the (0001) and $\{11\bar{2}2\}$ microfacets, but have different shape, depending on the mask geometries, which we currently believe is related to the V/III ratio. In pattern A, the window region occupies 75% of the entire patterned area, while in patterns B and C the windows occupy 50% and 25%, respectively. Because group III adatoms migrate from the SiO_2 mask region to the window region, the effective V/III ratio increases as the occupancy of the window region increases, that is, A>B>C. It was reported that lower V/III ratios promote the formation of $\{11\bar{2}2\}$ facets,[9] which is consistent with the present results.

Figure 1(d) shows the PL spectra from these microfacet QWs along with the PL spectrum from a planar QW for comparison. The CL measurements allowed each peak to be assigned to a microfacet. The main peak for pattern A at 510 nm originates from the (0001) microfacets and the peak position is the same as the planar QW. As demonstrated in Fig. 1(a), this is reasonable because the structure on pattern A consists of large (0001) facets, which can be regarded as planar (0001) planes. In addition to this main peak, a peak from the $\{11\bar{2}2\}$ facets appears at 430 nm. The difference in the emission color is due to the facet dependent In composition and the well layer thickness.[4] The emission from the $\{11\bar{2}2\}$ facets shifts toward longer wavelengths for patterns B and C, which can be understood by considering the migration of adatoms between facets. As noted in Ref. 4, Ga and In adatoms migrate from the $\{11\bar{2}2\}$ facets to the (0001) facets, and In more drastically migrates than Ga. Therefore, as the area of the (0001) facets increases, more In atoms escape from the $\{11\bar{2}2\}$ facets to the (0001) facets, which results in a smaller In composition on the $\{11\bar{2}2\}$ facets. It is also noteworthy that the migration of Ga and In adatoms produces intrafacet variations of the In composition particularly on the $\{11\bar{2}2\}$ facets.[4] As a result, the macroscopic emission line width of the $\{11\bar{2}2\}$ microfacet QWs became approximately 200 meV for both patterns B and C, which is ~50 meV larger than that of planar $\{11\bar{2}2\}$ QWs. Interestingly, just changing the mask geometry varies the emission color from green (pattern A) to blue (pattern B) through greenish blue (pattern C). This observation inspired the idea to combine different mask patterns for spectral syntheses using additive color mixtures.

Let us explain this idea using Fig. 2. Patterns A and B are schematically illustrated in Fig. 2(a). In addition, an example of a pattern mixture is shown where three periods of pattern A and one period of pattern B are mixed to form a new one period of 70 μm. (The mask pattern composed of m periods of pattern A and n periods of pattern B is denoted as A:B=m:n.) It is noteworthy that this new period is still smaller than the typical dimension of light emitting diodes (~300 μm square) and, therefore, the present proposal is applicable to practical devices. A bird's eye view of a microfacet InGaN/GaN QW grown on the mixed pattern drawn in Fig. 2(a) was taken by SEM and a typical image is shown in Fig. 2(b). As expected, the microfacet structures on patterns A and B [Figs. 1(a) and 1(b)] simultaneously appear according to the designed mask pattern. The local emission properties were assessed by CL mapping at RT viewed along the surface normal. Figure 2(c) shows CL images monitored at 420 and 520 nm, where a brighter contrast indicates a stronger emission. It is found that the $\{11\bar{2}2\}$ microfacet QWs emit at ~420 nm, while the (0001) microfacet QWs emit at ~520 nm, which is consistent with the PL shown in Fig. 1(d). The weaker CL from the (0001) microfacet QWs initially appears inconsistent with the PL, but this is due to the difference in the measurement configurations. The microscopically weaker emission from the (0001) microfacet QWs can be stronger macroscopically because the total area of the (0001) facets is much larger than that of the $\{11\bar{2}2\}$ facets.

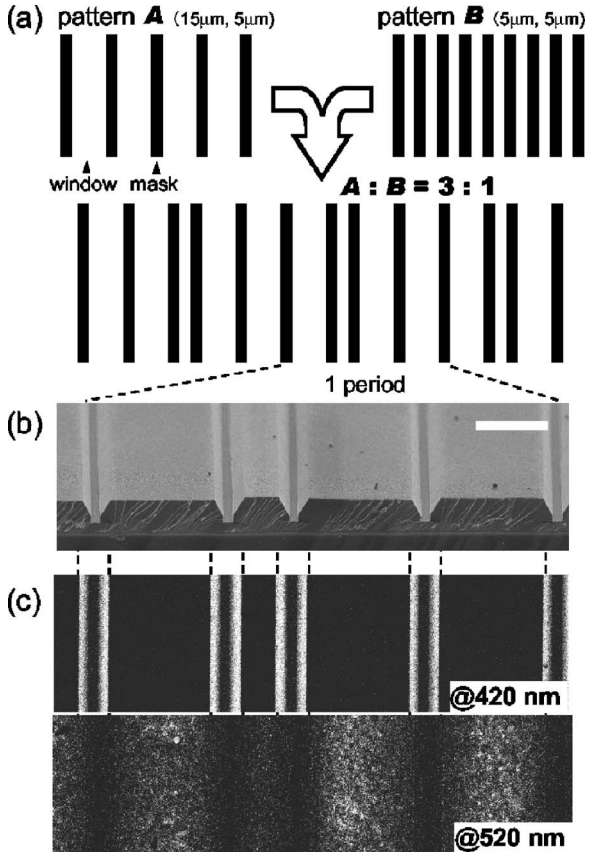

FIG. 2. (a) Schematic diagrams of mask patterns A and B, and an example of pattern mixture, which is composed of three periods of pattern A and one period of pattern B. The widths of (window, mask) for A and B are (15 μm, 5 μm) and (5 μm, 5 μm), respectively. (b) SEM image of a bird's-eye view of a microfacet structure fabricated on the mask pattern illustrated in (a). The scale bar represents 10 μm. (c) RT-CL images monitored at 420 and 520 nm.

The macroscopic optical properties of the microfacet QWs grown on mixed mask patterns were assessed by PL measurements at RT. Figure 3 shows the results for a series of samples grown on masks composed of patterns A and B with varying ratios. All the samples were formed on the same wafer, so that the influence of the growth conditions is negligible. It should be noted that pattern A results in emissions from both the (0001) and $\{11\bar{2}2\}$ facets, while pattern B results in an emission mostly from the $\{11\bar{2}2\}$ facets, as shown in Fig. 1(d). This tendency accounts for the spectral properties of the microfacet QWs on the designed patterns shown in Fig. 3. As the ratio of pattern A (B) increases, the emission from the (0001) ($\{11\bar{2}2\}$) facets becomes stronger, and con-

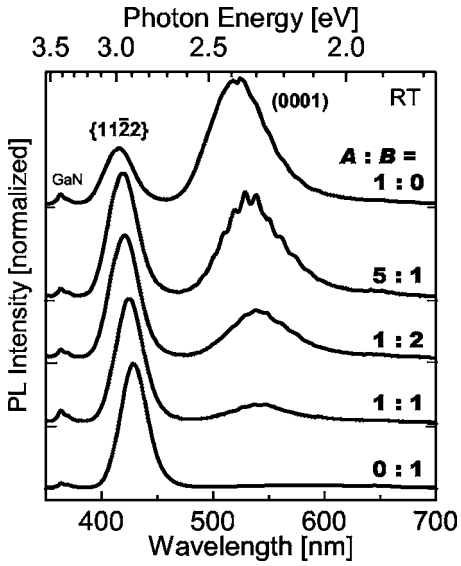

FIG. 3. PL spectra acquired at RT from InGaN/GaN microfacet QWs fabricated on various masks composed of patterns A and B with a ratio shown in the figure.

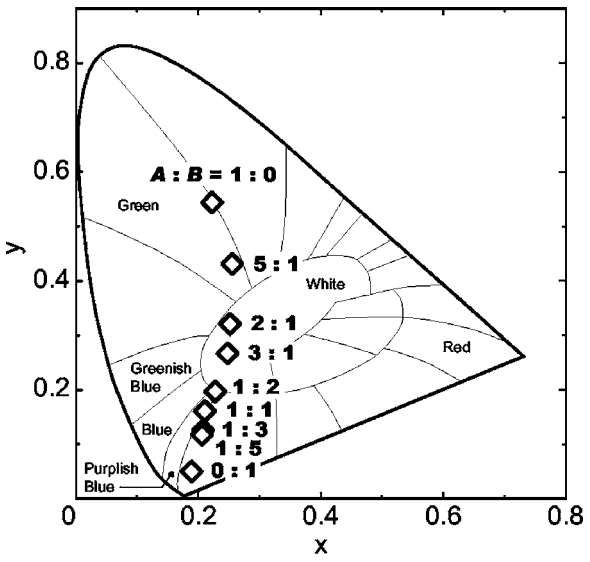

FIG. 4. CIE chromaticity diagram for the PL spectra shown in Fig. 3.

sequently, the apparent emission color changes.

The variation of the emission spectra due to the mask patterns shown in Fig. 3 are plotted in terms of the Commission Internationale de I'Eclairage (CIE) chromaticity diagram in Fig. 4 by which the variation of the apparent emission colors can be recognized. The emission color shifts from green (on pattern A) to purple (on pattern B) via white by changing the ratio of constituent patterns A and B. Monochromatic light from conventional LEDs should be on the boundary in the CIE chromaticity diagram. In contrast, the emissions of our microfacet QWs can be either close to or far from the boundary, depending on the design of the mask patterns.

In this study, we proposed to design mask patterns for regrowth in order to control the apparent emission color from InGaN/GaN microfacet QWs. It was demonstrated that properly designed mask patterns provide various three-dimensional microfacet structures and consequently, various emission colors from green to purple through white based on the additive color mixture. This observation leads us to believe that the proposed technique is promising for creating LEDs that emit an arbitrary color.

This work is partially supported by Grants for Regional Science and Technology Promotion from the Ministry of Education, Culture, Sports, Science and Technology, and the 21st Century COE Program (No. 14213201).

[1] J. Tsao, IEEE Circuits Devices Mag. **20**, 28 (2004).
[2] K. Nishizuka, M. Funato, Y. Kawakami, Sg. Fujita, Y. Narukawa, and T. Mukai, Appl. Phys. Lett. **85**, 3122 (2004).
[3] K. Nishizuka, M. Funato, Y. Kawakami, Y. Narukawa, and T. Mukai, Appl. Phys. Lett. **87**, 231901 (2005).
[4] M. Funato, T. Kotani, T. Kondou, Y. Kawakami, Y. Narukawa, and T. Mukai, Appl. Phys. Lett. **88**, 261920 (2006).
[5] V. Yu. Davydov, A. A. Klochikhin, R. P. Seisyan, V. V. Emtsev, S. V. Ivanov, F. Bechstedt, J. Furthmüller, H. Harima, A. V. Mudryi, J. Aderhold, O. Semchinova, and J. Graul, Phys. Status Solidi B **229**, R1 (2002).
[6] J. Wu, W. Walukiewicz, K. M. Yu, J. W. Ager III, E. E. Haller, H. Lu, and W. J. Schaff, Phys. Status Solidi B **240**, 412 (2003).
[7] H. Marchand, J. P. Ibbetson, P. T. Fini, S. Keller, S. P. DenBaars, J. S. Speck, and U. K. Mishra, J. Cryst. Growth **195**, 328 (1998).
[8] K. Hiramatsu, K. Nishiyama, M. Onishi, H. Mizutani, M. Narukawa, A. Motogaito, H. Miyake, Y. Iechika, and T. Maeda, J. Cryst. Growth **221**, 316 (2000).
[9] P. Fini, H. Marchand, J. P. Ibbetson, S. P. DenBaars, U. K. Mishra, and J. S. Speck, J. Cryst. Growth **209**, 581 (2000).